Journal of Environmental Radioactivity 152 (2016) 8–15

Contents lists available at ScienceDirect

Journal of Environmental Radioactivity

journal homepage: www.elsevier.com/locate/jenvrad

Distance to faults as a proxy for radon gas concentration in dwellings

Jean-Philippe Drolet*, Richard Martel

Institut national de la recherche scientifique, Eau Terre Environnement Centre (ETE-INRS), 490 de la Couronne, G1K 9A9, Canada

ARTICLE INFO

Article history:
Received 14 January 2015
Received in revised form
19 October 2015
Accepted 23 October 2015
Available online 28 November 2015

Keywords:
Radon potential
Fault
Geology
ANOVA
Sediment
Uranium

ABSTRACT

This research was done to demonstrate the usefulness of the local structural geology characteristics to predict indoor radon concentrations. The presence of geologic faults near dwellings increases the vulnerability of the dwellings to elevated indoor radon by providing favorable pathways from the source uranium-rich bedrock units to the surface. Kruskal–Wallis one-way analyses of variance by ranks were used to determine the distance where faults have statistically significant influence on indoor radon concentrations. The great-circle distance between the 640 spatially referenced basement radon concentration measurements and the nearest fault was calculated using the Haversine formula and the spherical law of cosines. It was shown that dwellings located less than 150 m from a major fault had a higher radon potential. The 150 m threshold was determined using Kruskal–Wallis ANOVA on: (1) all the basement radon measurements dataset and; (2) the basement radon measurements located on uranium-rich bedrock units only. The results indicated that 22.8% of the dwellings located less than 150 m from a fault exceeded the Canadian radon guideline of 200 Bq/m^3 when using all the basement radon measurements dataset. This percentage fell to 15.2% for the dwellings located between 150 m and 700 m from a fault. When using only the basement radon measurements located on uranium-rich bedrock units, these percentages were 30.7% (0–150 m) and 17.5% (150 m–700 m). The assessment and management of risk can be improved where structural geology characteristics base maps are available by using this proxy indicator.

1. Introduction

Radon is one of the six noble gases that occur naturally. Radon-222 (^{222}Rn), the most stable radon isotope, is an indirect radioactive product of uranium-238 (^{238}U). Consequently, the main sources of radon are the underlying rocks and soils (Borgoni et al., 2011; Hunter et al., 2009; IARC, 1988; Kochis and Leavitt, 1997; Nazaroff and Nero, 1988; Wattananikorn et al., 2008; Zhu et al., 1998). The alpha-particles emitted from the decaying of radon and its progenies represent the most important human exposure to ionizing radiation from environmental source (Cosma et al., 2013; Genay et al., 2006; Hauri et al., 2013). Epidemiological studies concluded that ^{222}Rn and some of its daughter elements (especially polonium-218 and polonium-214) are a major risk for lung cancer (Bochicchio, 2005; Darby et al., 2006) and are considered the second leading cause of lung cancer after tobacco smoking (WHO, 2009). Turner et al. (2011) noted a significant positive linear trend between lung cancer mortality and the categories of radon concentrations ($p = 0.02$) from the data of the American Cancer Society Cancer Prevention Study-II (CPS-II) prospective cohort. A 15% (95% confidence interval 1–31%) increase in the risk to die from lung cancer per each 100 Bq/m^3 radon was also observed. The 5-year survival rate for lung cancer is less than 20% (CCS, 2014).

In Canada, approximately 3261 cases of lung cancer are attributable to high indoor radon concentration exposure annually (Chen et al., 2012). Canadian public health authorities asked for maps of the radon potential to limit the radon exposure of its population. British Columbia (Branion-Calles et al., 2015; Rauch and Henderson, 2013), Ontario (Ford et al., 2014) and Nova Scotia (O'Reilly et al., 2013) prepared such radon risk maps along with a cross-Canada residential radon survey that collected approximately 14,000 indoor radon measurements (Health Canada, 2012; mapped in Hystad et al., 2014). In the Province of Quebec, an *Action plan about radon* was prepared by the Quebec intersectorial radon committee (QIRC). Effective in 2008, the main objectives were to develop a geogenic map of the radon potential for the Province of Quebec, to use the map as a preventive tool and to sensitize its population to the risk of high indoor radon concentration exposure. Drolet et al.

* Corresponding author.
E-mail address: jean-philippe.drolet@ete.inrs.ca (J.-P. Drolet).

http://dx.doi.org/10.1016/j.jenvrad.2015.10.023
0265-931X/

(2013) established positive proportion relationships between the bedrock units, the quaternary sediment deposits at the surface, the equivalent uranium concentrations from surface gamma-ray measurements, the uranium concentrations interpolated from geochemical surveys in sediments and 1417 basement radon concentration measurements in Quebec. The Quebec map of the radon potential based on radiogeochemical data was created using these relationships (Drolet et al., 2014).

This provincial-scale study was conducted to highlight radon-prone areas based on large scale predictors. The present paper focuses on the relevance of using local structural geology characteristics as complementary data to improve the radon potential map (prone areas). The research assumption is that using such complementary data should enhance the effectiveness of the predicted radon concentration in dwellings.

2. Material and methods

2.1. Available datasets

Four datasets were used: (1) major faults location, (2) bedrock units, (3) quaternary surficial deposits and (4) basement radon concentration measurements. The available airborne gamma-ray measurements of equivalent uranium concentration within the first 30 cm of earth surface and the uranium concentrations from geochemical surveys in lake and water course sediments were not included in this study because they are surficial surveys. The objectives of this study is to determine the relationships between indoor radon concentrations and the presence (or not) of a fault in the vicinity of the radon measurement points within or without uranium-rich bedrock units. The uranium surficial surveys mentioned above are not relevant for the study presented herein.

Both the fault locations and the bedrock unit base maps are available on SIGEOM, a georeferenced geoscientific database provided by the Ministère de l'Énergie et des Ressources naturelles of Québec. The surficial sediments base map is a combination of nine Quaternary geological maps (Dredge, 1983; Lamarche, 2011; Lasalle and Tremblay, 1978; Parent, 2014; St-Onge, 2009; Veillette, 1996; Veillette and Cloutier, 1993, 2014; Veillette et al., 2003). The basement radon concentration dataset was made of 3983 measurements from the ministère de la Santé et des Services sociaux (MSSS) (Fig. 1). This dataset is made of 3374 basement radon measurements performed by homeowners who asked for a radon test in their dwelling on a voluntary basis that was compiled by the Quebec Lung Association (QLA). Health Canada randomly sampled the other 609 dwellings all around the Province of Quebec for their basement radon concentrations. The basement radon concentrations were preferred than the measurements on other dwelling levels because they are generally higher and represent a worst case scenario. The radon concentrations in basements are also more directly related to the radon concentrations in the soil and bedrock that surrounds the dwellings foundations. The rate at which radon gas is diluted from basement to other floor levels is not necessarily constant depending on external factors such as the type of house and the indoor/outdoor air exchange. Using only the basement radon measurements ensures a more homogeneous dataset. These basement radon concentration measurements in dwellings are sparsely distributed over the entire province but show a higher density in highly populated areas such as Montréal, Québec City and Gatineau areas. The addresses of the basement radon measurements were geo-referenced using the G.O.LOC tool (Gestion des opérations de localisation et de cartographie). G.O.LOC. is a free application of the ministère de la Sécurité publique du Québec (MSP) that accurately transforms the input addresses into geographic coordinates.

2.2. Methodology

2.2.1. Calculation of the great-circle distances

The study was restricted to areas where the density of radon measurements was significant on an extended area and where detailed geological information including structural geology data were available. The objective was to verify if a correlation exists between radon gas concentrations in the basement of dwellings and distance to existing faults. The Communauté métropolitaine de Montréal (CMM) and the Communauté métropolitaine de Québec (CMQ) were the selected areas because they are the most populated of the Province of Quebec and have both the above cited selection criteria. The numerous measurements ensured that the distances between the faults and the basement radon measurements covered a wide range of values and were then statistically reliable. Having many measurements points in the vicinity of faults and also far from them strengthen the statistical robustness of the established relationships. The Gatineau area is a highly populated municipality that could have been included in the study, but most of the basement radon measurements in this zone are far from major faults. Also, there are not many uranium-rich bedrock units in the Gatineau area, so it was not relevant to add these data in the study. However, the basement radon measurements in the Gatineau area were used as a validation dataset to test the approach for the non-uranium-rich bedrock units.

The basement radon concentration measurements were superimposed on major faults identified on the geological base map using the ESRI's ArcGIS 10.1 environment (ESRI, 2012). The distance from the basement radon measurement point to the nearest fault was calculated using the NEAR function (Fig. 2). The distances calculated by this function are in the same units as the coordinate system of the input features (major fault location and basement radon concentration measurements). Using a geographic coordinate system leads to a calculated NEAR distance in decimal degrees (as opposed to linear units). However, the geographic coordinate system (NAD 1983) was chosen for the input datasets because they cover a large area. A projected coordinate system might involve distortion at large scale (Natural Resources Canada, 2014), so the calculated distance between the basement radon measurement points and the nearest fault might be erroneous. The ArcGIS NEAR function has the option to identify where in the fault polyline is the nearest coordinates to the basement radon measurements point.

The great-circle distances between the basement radon measurement points and the nearest fault point identified from the ArcGIS NEAR function were calculated from the modified Haversine formula (Eqs. (1) and (2)) (Robusto, 1957; Seema and Sheema, 2009) and the spherical law of cosines (Eq. (3)) (Chen et al., 2004). These equations assume a spherical earth and ignore the ellipsoidal effects, but are accurate approximations to calculate the distance between two points on earth knowing their coordinates.

$$D_{HAVERSINE} = 2R * a\,tan2\left(\sqrt{a},\ \sqrt{1-a}\right) \quad \text{(Eq. 1)}$$

$$\text{with } a = sin^2\left(\frac{\varnothing_2 - \varnothing_1}{2}\right) + cos\,(\varnothing_1)\,cos(\varnothing_2)\,sin^2\left(\frac{\lambda_2 - \lambda_1}{2}\right) \quad \text{(Eq. 2)}$$

$$D_{COSINES} = R*cos^{-1}[sin(\varnothing_1)\,sin(\varnothing_2) + cos(\varnothing_1)\,cos(\varnothing_2)\,cos(\lambda_2 - \lambda_1)] \quad \text{(Eq. 3)}$$

where D: distance between two points at the surface of earth (in m)

R: radius of the sphere

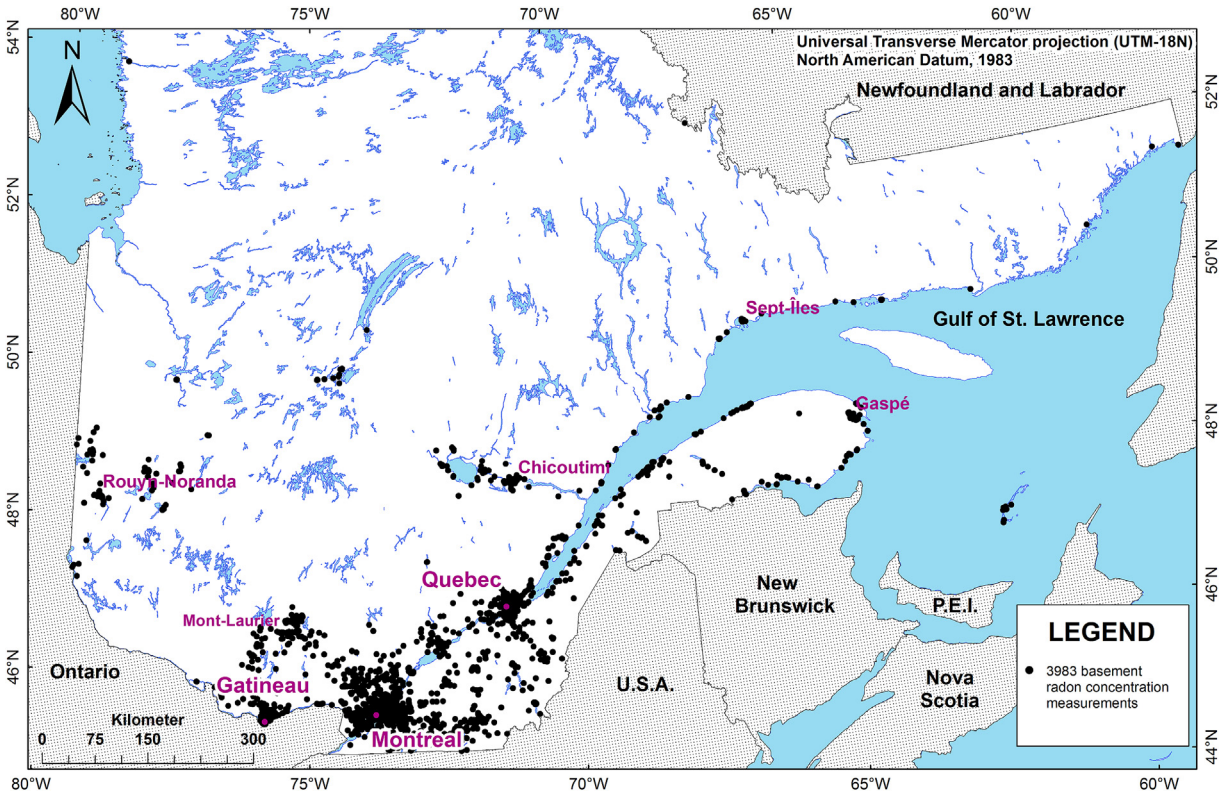

Fig. 1. Location of the 3983 basement radon concentration measurements in Quebec.

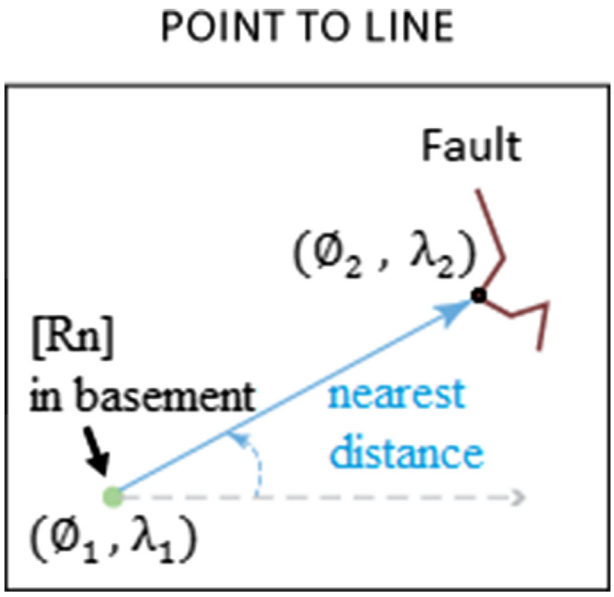

Fig. 2. ArcGIS NEAR function. The ($Ø_2$, λ_2) point is added when the user checks the option to add the coordinates of the two nearest points between the two features (modified from ESRI, 2014).

$Ø_1$, $Ø_2$: Latitude of points 1 and 2 (in radians)
λ_1, λ_2: Longitude of the points 1 and 2 (in radians).

2.2.2. Statistical analysis

Two approaches were investigated to determine the statistical relationship between the basement radon concentration measurements and the distance to faults. The first approach used all the radon concentration measurements dataset in the CMM and the CMQ areas. For the second approach, the statistical relationships were determined only for the basement radon measurement points located on high radon potential zones based on the bedrock units and the surficial deposits criteria. The basement radon measurement points located on non-uranium-rich bedrock units or located on more than 3 m of low permeability surficial deposits made of clay or silt were removed from the calculations. This second approach was made in order to test the effect of faults on basement radon concentrations in an environment where the generation of the radon gas by the bedrock is potentially high.

Fig. 3A shows the location of the basement radon concentration measurements and the faults in the CMM area whereas Fig. 3B shows these datasets in the CMQ. A total of 2264 basement radon measurement points were located in these two areas. The 2264 measurements were compared to the distances to the nearest fault to evaluate if the radon potential is higher in the vicinity of faults. Since the relationships between basement radon concentrations and geological indicators are not straight forward, (i.e. a small variation of the independent indicators are not necessarily associated with a proportional variation in radon concentration) (Drolet et al., 2013), the distances to faults were discretized in classes instead of working with a continuous dataset. Also, the statistical study included only the basement radon concentration measurements that were not further than 700 m from the nearest fault. The presence of a fault in the underlying ground has a major impact on the ^{222}Rn concentrations in soil gas. However, the lateral contribution of this favorable/permeable geological structure is less than 50 m each side of the fault (Ioannides et al., 2003; Swakoń et al., 2005; Varley and Flowers, 1993; Wiegand, 2001) (Fig. 4). Also, a multi-factor scoring system used 50 m as a threshold when determining the soil radon potential in Hong Kong (Tung et al.,

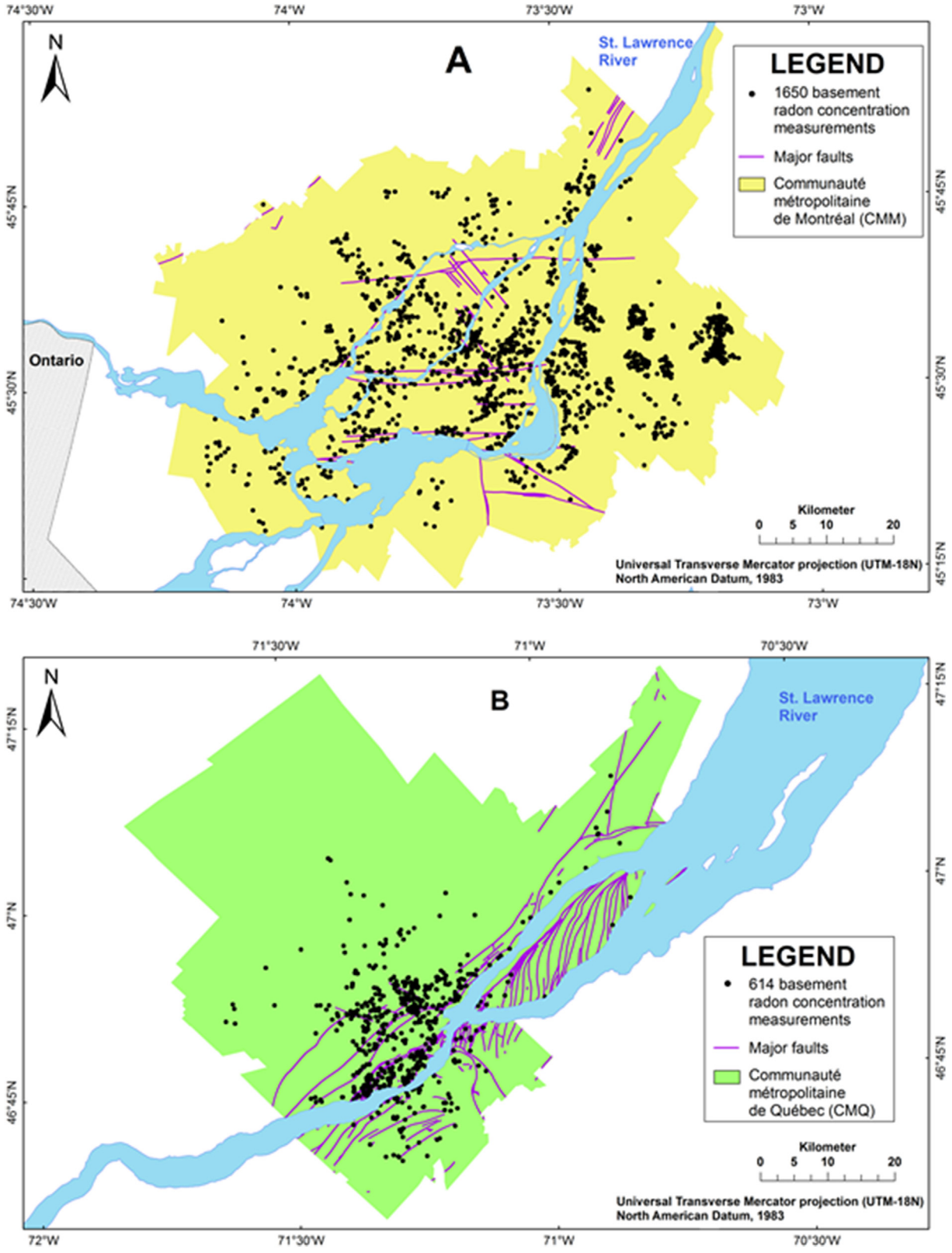

Fig. 3. Location of the basement radon concentration measurements and the major faults in (A) the communauté métropolitaine de Montréal (CMM) and (B) the communauté métropolitaine de Québec (CMQ).

2013). A larger range of distances between the radon measurement points and the faults were considered and extended to 700 m because multiple structural factors such as type of house, number of levels and indoor/outdoor air exchange also play a role in the indoor radon air levels (Hunter et al., 2009; Jelle, 2012; Kemski et al., 2001; Kropat et al., 2014). Finally, three conditions had to

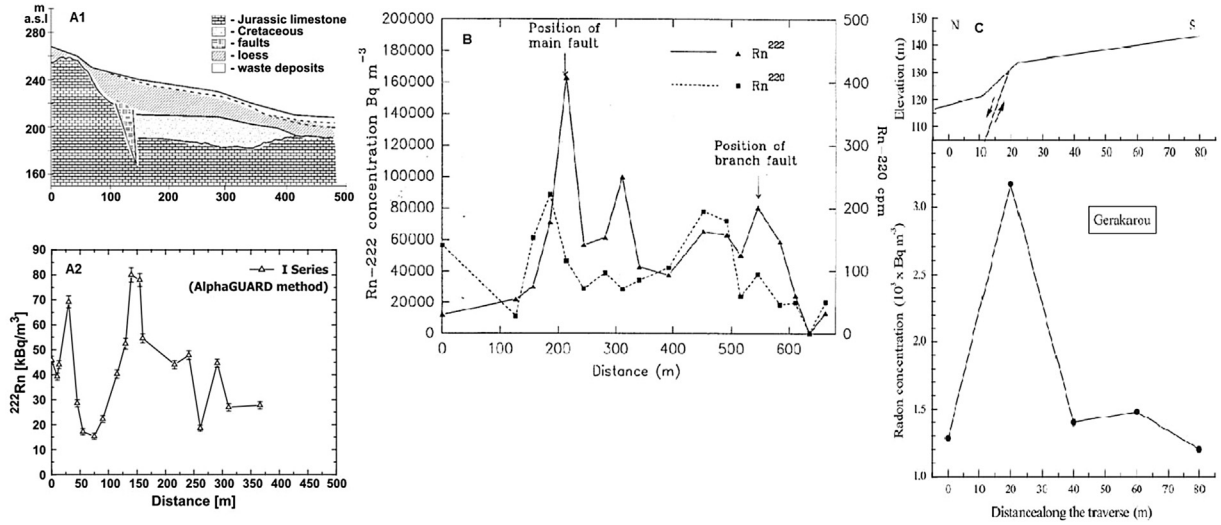

Fig. 4. Influence of the presence of a fault on ^{222}Rn concentrations in soil gas. (A1) Cross-section of the geology in the Krawkow area (Poland) and (A2) ^{222}Rn concentrations in soil gas along the profile shown in A1(modified from Swakoń et al., 2005); (B) ^{222}Rn concentrations in soil gas across the Sticklepath Fault II in SW England (modified from Varley and Flowers, 1993); (C) geological transect and ^{222}Rn profile across the Gerakarou fault in Greece (modified from (Ioannides et al., 2003).

be respected when discretizing the dependent criterion: (1) at least 50 basement radon concentration measurements were required per class to be statistically relevant; (2) classes had to encompass approximately the same number of radon measurements and; (3) classes had to cover approximately an equal range of distances to fault (modified from Drolet et al., 2013).

Kruskal–Wallis one-way analyses of variance on ranks (ANOVA) were performed on the basement radon concentration measurements within each class. One-way ANOVA have the capability to calculate the strength of the relationships between indoor radon concentrations and their dependent geological indicators (Smethurst et al., 2012; Drolet et al., 2013, 2014). The p-values calculated by the Kruskal–Wallis ANOVA allowed determining if the medians of the basement radon concentrations within each class were statistically similar or different than the ones within the other classes. A threshold of 0.05 for the p-value was set. A p-value above 0.05 meant that the compared classes shared a common median of basement radon concentrations. For the sake of simplicity, these classes will be stated as statistically similar because they represent a similar radon potential level. The two classes could then be merged together. The relationship between the basement radon concentrations within each class and the distances to fault were determined by calculating:

- the percentage of dwellings exceeding the Canadian radon guideline (200 Bq/m^3);
- the percentage of dwellings exceeding the radon immediate action level suggested by Health Canada (600 Bq/m^3) (Health Canada, 2014);
- the geometric mean (GM);
- the geometric standard deviation (GSD).

The second approach was done to verify if the relationship between the basement radon concentration measurements and the distance to fault was stronger when only using radon measurements located in a radon-prone area based on the bedrock units and the surficial deposits. As a daughter element of ^{238}U, ^{222}Rn indoor concentration is more likely higher where uranium-rich bedrock units are present. Potentially uranium-rich bedrock units across Quebec were presented in Drolet et al. (2013). The type and the thickness of the surficial deposits are also related to the indoor radon levels. The radon gas generated by the underground sources (uranium-rich bedrocks) must migrate through the soil and reach the dwellings before decaying into his daughter element to have an influence on the indoor radon concentration level. It is known that fine grained surficial deposits like clay and silt create a barrier to the vertical migration of radon gas (Alexander and Devocelle, 1997; Miles and Ball, 1996). A uranium-rich bedrock unit not capped by a silt/clay barrier was considered as a radon-prone area from a geological point of view. If the silt/clay barrier was thinner than 3 m, it was not considered a barrier because most of the overburden will be removed by excavation during dwelling construction. Drolet et al. (2013) combined the source parameter (uranium-rich bedrock units) and the migration parameter (surficial deposits) into a geology criterion.

The same methodology described previously (creating classes, testing the statistical similarities from Kruskal–Wallis ANOVA) were performed on the basement radon concentration measurements located in radon-prone areas based on the geology criterion. The hypothesis was that the influence of the distance to fault might be more important in zones where a more important source of radon is present in bedrock. The effect of the presence of a natural migration pathway (faults) on indoor radon concentrations was more directly tested where the soil gas radon concentrations tended to be higher. The effect of a fault where the bedrock is non-uranium-rich might only add noise to the statistical model.

3. Results

3.1. Calculation of the great-circle distances

The results obtained for all the 2264 radon measurements points are not presented herein to avoid redundancy. The two formulas give approximatively the same great-circle distances. The maximum Δ distance between the Haversine formula and the spherical law of cosines was 1.083×10^{-3} m.

3.2. Statistical analysis

The first statistical analysis included the all-basements radon concentration dataset, whether they are located in a high radon potential level area or not (based on the geology criterion) (Table 1).

Table 1
Kruskal–Wallis one-way ANOVA on ranks on the five classes of distances between the basement radon concentration points and the nearest fault. The median of basement radon concentration (Bq/m^3) was added in parenthesis. Bold characters are for classes that have a p-value above the threshold of 0.05.

Compared class 1 (median)	Compared class 2 (median)	p-value
0–75 m (85)	**75–150 m (78)**	**0.564**
0–75 m (85)	150–300 m (72)	0.048
0–75 m (85)	300–500 m (70)	0.043
0–75 m (85)	500–700 m (56)	0.001
75–150 m (78)	**150–300 m (72)**	**0.232**
75–150 m (78)	**300–500 m (70)**	**0.194**
75–150 m (78)	500–700 m (56)	0.013
150–300 m (72)	**300–500 m (70)**	**0.937**
150–300 m (72)	**500–700 m (56)**	**0.120**
300–500 m (70)	**500–700 m (56)**	**0.126**

The Kruskal–Wallis one-way ANOVA on ranks is a non-parametric test. This test was chosen because the radon concentration dataset are not from a normally distributed population (tested by Shapiro–Wilk tests). A p-value calculated by the Kruskal–Wallis ANOVA above 0.05 means that the assumption that the two compared classes shared a common median cannot be rejected at the 95% confidence level, i.e. they include basement radon concentrations that are statistically similar.

The “0–75 m” and “75–150 m” classes were merged because they presented a statistically similar median radon potential based on a high p-value of 0.564. The “75–150 m” class also had statistical similarities with the “150–300 m” and “300–500 m” classes, but it was more strongly related to the “0–75 m” class based on a higher p-value (0.564 vs 0.232 and 0.194). Also, there were 22.9% and 22.8% of the basement radon concentration measurements that exceeded the Canadian radon guideline of 200 Bq/m^3 in the “0–75 m” and “75–150 m” classes respectively (not shown in the table). These percentages drop to 15.2% for the “150–300 m” class and 17.0% for the “300–500 m” class. The strength of the statistical relationship is then more important between the first two classes. Proceeding with the same methodology led to merging the “150–300 m”, “300–500 m” and “500–700 m” classes together based on the calculated p-values. As a lexical distinction, classes were renamed as a “group” after being merged. The two statistical different groups created from the Kruskal–Wallis one-way ANOVA on ranks are presented in Table 2.

The 540 basement radon concentration measurements were located in radon-prone areas based on the geology criterion suggested by Drolet et al. (2013, 2014) (358 in the CMM and 182 in the CMQ). Only 212 measurements are closer than 700 m from the nearest fault. Three classes of distances were created to respect the three conditions cited above in the 2.2.2 section: “0–150 m”, “150–300 m” and “300–700 m”. Table 3 shows the results of the Kruskal–Wallis one-way ANOVA on ranks when comparing the three classes. The “150–300 m” was statistically similar to the “0–150 m” and “300–700 m” classes based on p-values above 0.05. However, the statistical relationship between the basement radon concentration measurements within the “150–300 m” and “300–700 m” classes was notably stronger having a p-value of 0.882 against a p-value of 0.094 when comparing the “0–150 m” and “150–300 m” classes. The percentage of basement radon concentration measurements that exceeded the Canadian radon guideline of 200 Bq/m^3 was also more similar for the two farthest distance classes (18.6% and 16.7% compared to 30.7% for the “0–150 m” class). The “150–300 m” and “300–700 m” classes were merged for these reasons. The descriptive statistics and the Kruskal–Wallis one-way ANOVA results when comparing the “0–150 m” class and the “150–700 m” group are shown in Table 4.

Table 3
Kruskal–Wallis one-way ANOVA on ranks on the three classes of distances between the basement radon concentration points and the nearest fault. The median of basement radon concentration (Bq/m^3) was added in parenthesis. Bold characters are for classes that have a p-value above the threshold of 0.05.

Compared class 1 (median)	Compared class 2 (median)	p-value
0–150 m (89)	**150–300 m (59)**	**0.094**
0–150 m (89)	300–700 m (63)	0.026
150–300 m (59)	**300–700 m (63)**	**0.882**

4. Discussion

The faults are mapped from different techniques depending on the geological context. Faults can be mapped from direct field observations where the bedrock outcrops. Breccia will indicate the presence of a fault and its location will be determined from GPS. Deeper faults covered by surficial deposits were mapped based on the discontinuities of the physical properties measured from geophysical surveys (seismic methods and aeromagnetic surveys) and the log data. The precision of all these methods is approximately in the meter range. The radon measurement points also have uncertainties in the meter range caused by the georeferencing of the addresses. The maximum Δ distances, in absolute value, is 1.8 mm so both equations could be used for the purpose of this study.

The Kruskal–Wallis one-way ANOVA on rank indicated that the dwellings located within 150 m from the nearest major fault were in an area where the radon potential was higher. Medians, 25th and 75th percentiles, geometric means and percentages of basements radon measurements above the Canadian radon guideline are higher within that range (Tables 2 and 4). For Strand et al. (2005), an area where 20% of the radon concentration measurements exceed 200 Bq/m^3 was considered a high-risk zone in Norway. Our study determined that the buffer zone on 150 m each side of a major fault has a high radon potential: 22.8% of the basement radon measurements within 150 m from a fault were above the Canadian radon guideline of 200 Bq/m^3 in the CMM and the CMQ when considering the all-measurement dataset. This percentage rose to 30.7% for the basement radon measurements located in radon-prone areas based on the geology criterion. The difference is caused by the presence of a uranium-rich bedrock unit (potential

Table 2
Descriptive statistics and Kruskal–Wallis one-way ANOVA on two groups of distances between the basement radon measurement points and the nearest fault. All the basement radon measurement dataset of the CMM and the CMQ was included for these calculations.

Group (x in m)	n	Median (Bq/m^3)	25th Percentile (Bq/m^3)	75th Percentile (Bq/m^3)	GM (Bq/m^3)	GSD (Bq/m^3)	% [Rn] ≥ 200 Bq/m^3	% [Rn] ≥ 600 Bq/m^3
0 < x < 150	206	81	43	190	88	2.6	22.8	1.0
150 ≤ x < 700	434	67	33	137	69	2.7	15.2	1.4

$\chi^2 = 8.899$ with 1 degree of freedom. (p-value between two groups = 0.003; statistically significant difference)x: distance between dwelling and fault.
GM: geometric mean.
GSD: geometric standard deviation.
% [Rn] ≥: percentage of dwellings above the criteria below.

Table 4
Descriptive statistics and Kruskal–Wallis one-way ANOVA on one group and one class of distances between the radon measurement points and the nearest fault. Only the basement radon concentration measurements located in high radon potential areas based on the geology criterion were included for the calculations presented herein.

Group (y in m)	n	Median (Bq/m^3)	25th Percentile (Bq/m^3)	75th Percentil (Bq/m^3)	GM (Bq/m^3)	GSDm (Bq/m^3)	% [Rn] ≥ 200 Bq/m^3	% [Rn] ≥ 600 Bq/m^3
$0 < y < 150$	75	89	37	226	93	3.0	30.7	2.7
$150 \leq y < 700$	137	59	26	137	66	2.9	17.5	2.2

$\chi^2 = 5.297$ with 1 degree of freedom. (p-value between two groups = 0.021; statistically significant difference)y: distance between dwelling and fault.
GM: geometric mean.
GSD: geometric standard deviation.
% [Rn] ≥: percentage of dwellings above the criteria below.

radon source) in the subsurface for the second approach. In the first case, some dwellings were located in the vicinity of a fault, but there was less radon emission by the underlying bedrocks. The faults are a favorable pathway for radon gas migration, but the gas migrating through it by diffusion/advection/convection has a low radon concentration, thus resulting in lower indoor radon concentrations in the surrounding dwellings.

The Gatineau area was used to validate the 150 m thresholds. As mentioned previously, the Gatineau area is populous, but most of the basement radon measurements are far from faults and were not included in the main core of the statistical study. However, 4 of the 12 dwellings (33.3%) located less than 150 m from the nearest fault in the Gatineau area exceeded 200 Bq/m^3 in this zone. In the 150–700 m range, only 6 basement radon measurements exceeded 200 Bq/m^3 on the 36 dwellings found (16.7%). These two ratios are in accordance with those found in the CMM and the CMQ areas. Note that the 48 basement radon measurements in the Gatineau area were located on non-uranium-rich bedrock units.

The descriptive statistics in Tables 2 and 4 confirm the hypothesis that the influence of the distance to fault is more important in radon-prone areas based on the geology criterion. The differences in medians, 25th and 75th percentiles, geometric means and percentages of basements radon measurements above the Canadian radon guidelines were greater when considering only the basement radon concentration measurements where a uranium-rich bedrock unit was present. The occurrence of faults in the near environment (<150 m) had a greater influence on indoor radon concentrations in this case. A p-value of 0.021 calculated with the Kruskal–Wallis ANOVA confirmed that the radon potential associated to the "0–150 m" class was statistically different than the one of the "150–700 m" group.

A p-value of 0.003 was calculated from the Kruskal–Wallis ANOVA when using all the basement radon measurement dataset. The p-values calculated from the two methodologies (0.003 and 0.021) confirmed that the basement radon concentration measurements located within 150 m from the nearest fault were statistically different from the radon measurements farther away. This indicates that there were statistical differences in the medians of radon measurements among the compared groups, i.e. the hypothesis that the compared groups share a common median can be rejected and the statistical differences were not due to random sampling variability. The areas within 150 m on each side of a fault could be used as an aggravating indicator for the radon potential. Ielsch et al. (2010) applied this strategy when determining the geogenic radon potential in Bourgogne (France).

5. Conclusion

The Kruskal–Wallis one-way ANOVA on ranks established the relationships between the basement radon concentration measurements based on their distances to the nearest fault. The distances from the nearest fault were discretized in classes. The statistical relationships of the radon measurements within each class were calculated and statistically similar classes were then merged. A threshold of 150 m was determined as the cut-off value where the radon potential based on the distance from the nearest fault rises significantly. The relationships between the basement radon concentration measurements and the distance to the nearest fault found in the present study played a major role in a radon assessment and management risk context. The Quebec public health authorities could use the available structural geology base maps as a complementary tool to the geogenic map of the radon potential already in use (Drolet et al., 2014). The areas near a favourable/permeable pathway to radon migration should be of concern to promote collection of indoor radon measurements and mitigation actions regardless of the determined geogenic radon potential level. Zones of high geogenic radon potential within 150 m of a fault are of great importance as approximately 1 dwelling out of 3 exceeds the Canadian radon guideline when built on uranium-rich bedrock units and approximately 1 dwelling out of 4 without uranium-rich bedrock units. In comparison, less than 1 dwelling out of 5 (18.7% exactly) exceeds 200 Bq/m^3 in the actual Province of Quebec dataset. The basement radon measurements in the vicinity of a fault (<150 m) are then more prone to high levels. The structural geology characteristics base maps should be included in models when mapping the geogenic radon potential.

Acknowledgment

The authors thank the ministère de la Santé et des Services sociaux du Québec and the Institut national de santé publique du Québec for partly funding this research. We would also like to thank them for sharing the indoor radon measurements dataset. The authors are grateful to the Ministère de l'Énergie et des Ressources naturelles (Gouvernement du Quebec) for sharing their geological data. Finally, we thank M. Denis Lavoie, from the Geological Survey of Canada (GSC-Quebec), for his inputs on the methodologies used to locate the faults in Quebec and Pr. André St-Hilaire of INRS-ETE for his support in the statistical analysis.

References

Alexander, W.G., Devocelle, L.L., 1997. Mapping indoor radon potential using geology and soil permeability. In: 1997 International Radon Symposium, pp. 4.1–4.16.
Bochicchio, F., 2005. Radon epidemiology and nuclear track detectors: methods, results and perspectives. Radiat. Meas. 40, 177–190.
Borgoni, R., Tritto, V., Bigliotto, C., de Bartolo, D., 2011. A geostatistical approach to assess the spatial association between indoor radon concentration, geological features and building characteristics: the case of Lombardy, Northern Italy. Int. J. Environ. Res. Public Health 8, 1420–1440.
Branion-Calles, M.C., Nelson, T.A., Henderson, S.B., 2015. A geospatial approach to the prediction of indoor radon vulnerability in British Columbia, Canada. J. Expo. Sci. Environ. Epidemiol. 1–12.
Canadian Cancer Society (CCS), 2014. Lung cancer Statistics. Available at: https://www.cancer.ca/en/cancer-information/cancer-type/lung/statistics/?region=qc (accessed 19.09. 14.).
Chen, C.L., Hsu, T.P., Chang, J.R., 2004. A novel approach to great circle sailings: the great circle equation. J. Navig. 57, 311–325.
Chen, J., Moir, D., Whyte, J., 2012. Canadian population risk of radon induced lung

cancer: a re-assessment based on the recent cross-Canada radon survey. Radiat. Prot. Dosim. 152, 9–13.
Cosma, C., Cucos, A., Dicu, T., 2013. Preliminary results regarding the first map of residential radon in some regions in Romania. Radiat. Prot. Dosim. 155, 343–350.
Darby, S., Hill, D., Deo, H., Auvinen, A., Barros-Dios, J.M., Baysson, H., Bochicchio, F., Falk, R., Farchi, S., Figueiras, A., Hakama, M., Heid, I., Hunter, N., Kreienbrock, L., Kreuzer, M., Lagarde, F., Mäkeläinen, I., Muirhead, C., Oberaigner, W., Pershagen, G., Ruosteenoja, E., Scaffrath Rosario, A., Tirmarche, M., Tomášek, L., Whitley, E., Wichmann, H.E., Doll, R., 2006. Residential radon and lung cancer - detailed results of a collaborative analysis of individual data on 7148 persons with lung cancer and 14,208 persons without lung cancer from 13 epidemiologic studies in Europe. Scand. J. Work Enviorn. Health 32, 1–84.
Dredge, L.A., 1983. Surficial geology, Sept-Iles, Quebec/Géologie de surface, Sept-Îles, Québec. Geological Survey of Canada. "A" Series Map 1575A.
Drolet, J.P., Martel, R., Poulin, P., Dessau, J.C., 2014. Methodology developed to make the Quebec indoor radon potential map. Sci. Total Environ. 473–474, 372–380.
Drolet, J.P., Martel, R., Poulin, P., Dessau, J.C., Lavoie, D., Parent, M., Lévesque, B., 2013. An approach to define potential radon emission level maps using indoor radon concentration measurements and radiogeochemical data positive proportion relationships. J. Environ. Radioact. 124, 57–67.
Environmental Systems Research Institue (ESRI), 2014. Near (Analysis). Available at: http://help.arcgis.com/en/arcgisdesktop/10.0/help/index.html#//00080000001q000000 (accessed 22.09. 14.).
Environmental Systems Research Institute (ESRI), 2012. ArcMap 10.1. ESRI, Redlands, CA.
Ford, K., et al., 2014. Radon Geologically Based Potential Map of Southern Ontario. Natural Resources Canada (Preliminary map under revision).
Genay, Y., Millot, I., Navillon, B., Fiet, C., 2006. Le risque radon en Bourgogne. Observatoire Régional de la Santé, Bourgogne.
Hauri, D.D., Huss, A., Zimmermann, F., Kuehni, C.E., Röösli, M., 2013. Prediction of residential radon exposure of the whole Swiss population: comparison of model-based predictions with measurement-based predictions. Indoor Air 23, 406–416.
Health Canada, 2012. Cross-Canada Survey of Radon Concentrations in Homes, Final Report. Available at: http://www.hc-sc.gc.ca/ewh-semt/alt_formats/pdf/radiation/radon/survey-sondage-eng.pdf (accessed 09.12.14.).
Health Canada, 2014. Government of Canada Radon Guideline. Available at: http://www.hc-sc.gc.ca/ewh-semt/radiation/radon/guidelines_lignes_directrice-eng.php (accessed 08.12.14.).
Hunter, N., Muirhead, C.R., Miles, J.C.H., Appleton, J.D., 2009. Uncertainties in radon related to house specific factors and proximity to geological boundaries in England. Radiat. Prot. Dosim. 136, 17–22.
Hystad, P., Brauer, M., Demers, P.A., Johnson, K.C., Setton, E., Cervantes-Larios, A., Poplawski, K., McFarlane, A., Whitehead, A., Nicol, A.M., 2014. Geographic variation in radon and associated lung cancer risk in Canada. Can. J. Public Health 105, e4–e10.
Ielsch, G., Cushing, M.E., Combes, P., Cuney, M., 2010. Mapping of the geogenic radon potential in France to improve radon risk management: methodology and first application to region Bourgogne. J. Environ. Radioact. 101, 813–820.
International Agency for Research on Cancer (IARC), 1988. Monographs on the evaluation of carcinogenic risks to humans. In: Man-made Mineral Fibres and Radon, vol. 43. Lyon.
Ioannides, K., Papachristodoulou, C., Stamoulis, K., Karamanis, D., Pavlides, S., Chatzipetros, A., Karakala, E., 2003. Soil gas radon: a tool for exploring active fault zones. Appl. Radiat. Isot. 59, 205–213.
Jelle, B.P., 2012. Development of a model for radon concentration in indoor air. Sci. Total Environ. 416, 343–350.
Kemski, J., Siehl, A., Stegemann, R., Valdivia-Manchego, M., 2001. Mapping the geogenic radon potential in Germany. Sci. Total Environ. 272, 217–230.
Kochis, N.S., Leavitt, S.W., 1997. Radon emanation from soil of Kenosha, Racine and Waukesha Counties, Southeastern Wisconsin. Geosci. Wis. 16, 55–62.
Kropat, G., Bochud, F., Jaboyedoff, M., Laedermann, J.P., Murith, C., Palacios, M., Baechler, S., 2014. Major influencing factors of indoor radon concentrations in Switzerland. J. Environ. Radioact. 129, 7–22.
Lamarche, L., 2011. Évolution paléoenvironnementale de la dynamique quaternaire dans la région de Québec: Application en modélisation tridimensionnelle et hydrogéologique. Université du Québec (ETE-INRS) (Philosophiae Doctor thesis).
Lasalle, P., Tremblay, G., 1978. Dépôts Meubles-Saguenay-Lac-Saint-Jean, vol. 191. Ministère des richesses naturelles. Direction générale de la recherche géologique, Rapport géologique.
Miles, J., Ball, K., 1996. Mapping radon-prone areas using house radon data and geological boundaries. Environ. Int. 22, S779–S782.
Natural Resources Canada, 2014. The UTM Grid – Map Projections. Available at: http://www.nrcan.gc.ca/earth-sciences/geography/topographic-information/maps/9775 (accessed 28.09.14.).
Nazaroff, W.W., Nero, A.V., 1988. Radon and its Decay Products in Indoor Air. John Wiley and Sons, New York.
O'Reilly, G.A., Goodwin, T.A., McKinnon, J.S., Fisher, B.E., 2013. Map Showing the Potential for Radon in Indoor Air in Nova Scotia. Nova Scotia Department of Natural Resources, Mineral Resources Branch, pp. 2013–2028. Open File Map ME.
Parent, M., 2014. Géologie des formations superficielles du Québec méridional. Geological Survey of Canada (Preliminary map under revision).
Rauch, S.A., Henderson, S.B., 2013. A comparaison of two methods for ecologic classification of radon exposure in British Columbia: residential observations and the radon potential map of Canada. Can. J. Public Health 104, e240–e245.
Robusto, C.C., 1957. The Cosine-Haversine formula. Am. Math. Mon. 64, 38–40.
Seema, S.R., Sheema, A., 2009. Dynamic bus arrival time prediction using GPS data. In: 10th National Conference on Technological Trends (NCTT09), pp. 193–197. Kerala.
Smethurst, M.A., Watson, R.J., Finne, I., Ganerod, G.V., Rudjord, A.L., 2012. Norwegian bedrock and drift geology as a predictor of indoor radon concentrations. In: 11th International Workshop on the Geological Aspects of Radon Risk Mapping (Prague).
St-Onge, D.A., 2009. Surficial geology, lower Ottawa Valley, Ontario-Quebec/Géologie des formations en surface, basse vallée de l'Outaouais, Ontario-Québec. Geological Survey of Canada. "A" Series Map 2140A.
Strand, T., Lunder Jensen, C., Ånestad, K., Ruden, L., Beate Ramberg, G., 2005. High radon areas in Norway. Int. Congr. Ser. 1276, 212–214.
Swakoń, J., Kozak, K., Paszkowski, M., Gradziński, R., Łoskiewicz, J., Mazur, J., Janik, M., Bogacz, J., Horwacik, T., Olko, P., 2005. Radon concentration in soil gas around local disjunctive tectonic zones in the Krakow area. J. Environ. Radioact. 78, 137–149.
Tung, S., Leung, J.K.C., Jiao, J.J., Wiegand, J., Wartenberg, W., 2013. Assessment of soil radon potential in Hong Kong, China, using a 10-point evaluation system. Environ. Earth Sci. 68, 679–689.
Turner, M.C., Krewski, D., Chen, Y., Pope, C.A., Gapstur, S., Thun, M.J., 2011. Radon and lung cancer in the American Cancer Society cohort. Cancer Epidem. Biomar. 20, 438–448.
Varley, N.R., Flowers, A.G., 1993. Radon in soil gas and its relationship with some major faults of SW England. Environ. Geochem. Health. 15, 145–151.
Veillette, J.J., 1996. Géomorphologie et géologie du Quaternaire du Témiscamingue, Québec et Ontario. In: Bulletin, vol. 476. Geological Survey of Canada.
Veillette, J.J., Cloutier, M., 1993. Géologie des formations en surface, Gaspésie. Geological Survey of Canada, Québec. "A" Series Map 1804A.
Veillette, J.J., Cloutier, M., 2014. Géologie du Quaternaire dans le Bas-Saint-Laurent. Geological Survey of Canada, Québec (Preliminary map under revision).
Veillette, J.J., Paradis, S.J., Thibaudeau, P., 2003. Les cartes de formations en surface de l'Abitibi. Geological Survey of Canada, Québec. Open File 1523.
Wattananikorn, K., Emharuthai, S., Wanaphongse, P., 2008. A feasibility study of geogenic indoor radon mapping from airborne radiometric survey in northern Thailand. Radiat. Meas. 43, 85–90.
Wiegand, J., 2001. A guideline for the evaluation of the soil radon potential based on geogenic and anthropogenic parameters. Environ. Geol. 40, 949–963.
World Health Organization (WHO), 2009. Fact Sheet No 291: Radon and cancer. Available at: http://www.who.int/mediacentre/factsheets/fs291/en/ (accessed 02.12.14.).
Zhu, H.C., Charlet, J.M., Tondeur, F., 1998. Geological controls to the indoor radon distribution in southern Belgium. Sci. Total Environ. 220, 195–214.